NREL/TP-451-5813 • UC Category: 273 • DE94000201

Thin Film Cadmium Telluride Photovoltaic Cells

Annual Subcontract Report 1 November 1991 – 31 October 1992

A. D. Compaan, R. G. Bohn
University of Toledo
Toledo, Ohio

NREL technical monitor: B. von Roedern

National Renewable Energy Laboratory
1617 Cole Boulevard
Golden, Colorado 80401-3393
Operated by Midwest Research Institute
for the U.S. Department of Energy
under Contract No. DE-AC02-83CH10093

Prepared under Subcontract No. ZN-1-19019-3

October 1993

NOTICE

Printed in the United States of America
Available from:
National Technical Information Service
U.S. Department of Commerce
5285 Port Royal Road
Springfield, VA 22161

Price: Microfiche A01
Printed Copy A03

Codes are used for pricing all publications. The code is determined by the number of pages in the publication. Information pertaining to the pricing codes can be found in the current issue of the following publications which are generally available in most libraries: *Energy Research Abstracts (ERA); Government Reports Announcements and Index (GRA and I); Scientific and Technical Abstract Reports (STAR)*; and publication NTIS-PR-360 available from NTIS at the above address.


Printed on recycled paper

DISCLAIMER

Portions of this document may be illegible electronic image products. Images are produced from the best available original document.

Summary

The major objectives of this program at the University of Toledo are the development and optimization of radio-frequency (rf) sputtering and laser-driven physical vapor deposition (LDPVD) for CdTe-based thin-film solar cells. Both of these techniques are vacuum-based and share several other common physical principles. They may differ somewhat in the typical kinetic energies of Cd, Te, and S which impact on the growth surface. The values of several of the processing parameters which have been optimized with the LDPVD technique have been taken as starting values for the rf sputtering method. During this year we have completed an initial optimization of the sputtering parameters for CdTe growth and also have successfully sputtered CdS for the first time in our laboratory. In addition, we have fabricated successfully what we believe are the first CdS/CdTe cells in which rf sputtering was used for both CdS and CdTe layers. By the end of the second contract year we have achieved an all-LDPVD cell with an AM1.5 efficiency of 10.5% and an all-rf-sputtered cell with AM1.5 efficiency of 10.4% as tested by NREL.

During the second year, some adjustments have been made to the LDPVD process for cell fabrication including slightly higher growth temperature, slightly shorter anneal time after $CdCl_2$ treatment, and shorter diffusion times after contact evaporation. A variety of characterization measurements have been essential in making progress in cell efficiency from 8.7% to 10.5% over the past year. These include: SEM, SEM/EDS, photoluminescence, Raman, Hall conductivity measurements, and I-V, SQE, and OBIC measurements of cell parameters.

Table of Contents

1.0 Introduction

1.1 Background

This project began in July of 1990 as a joint project with the University of Toledo as the lead institution and the close participation of two lower tier subcontractors, Solar Cells Inc (SCI), and Glasstech Solar Inc (GSI). Near the end of 1990 GSI ceased operations and terminated its participation in the contract. Meanwhile, Solar Cells' time scale for moving toward module production advanced more rapidly than projected and NREL negotiated a separate contract with SCI in the spring of 1991. The contract with UT was renegotiated to reflect these changes with SCI remaining as a lower tier subcontractor only through the end of the first contract year. The time allocated for the first award year was extended through October 1991 to allow the University of Toledo to pick up some of the work initially planned for GSI. The University of Toledo contract was modified to reduce the second and third year emphasis on scale-up to commercialization, but retained the emphasis on basic science and the further development of the laser deposition and rf sputtering processes.

During the second year, the UT group placed increasing emphasis on optimization of the rf sputtering method for deposition of thin films of CdTe and CdS. Although official participation of SCI in this project has ceased, we have maintained considerable communication and frequent collaboration with SCI. This involved the occasional exchange of thin films, cooperation in the use of facilities including at SCI a stylus profilometer and calibrated solar standard, and at UT the rf sputtering system. Students or faculty at UT assisted in film growth by sputtering, double-beam optical absorption measurements, Raman and photoluminescence measurements, and Hall measurements.

1.2 Technical Approach

The UT group has studied intensively the laser-driven physical vapor deposition process (LDPVD) for CdS/CdTe cell fabrication. The LDPVD process combines the advantages of (ultra)high vacuum cleanliness and monolayer control over the growth interface. It has many similarities to molecular beam epitaxy with much less cost. This growth process was studied intensively during the first contract year during which complete CdS/CdTe solar cells were fabricated with NREL-tested efficiencies up to 8.7%.[1,2] During the second year a variety of adjustments were made to the LDPVD process and to the post-deposition processing which have yielded an NREL-tested efficiency of 10.5%.

Although the LDPVD technique has permitted convenient control over target fabrication, since small cold-pressed targets could be used, the method appears difficult to scale up for economical deposition of m^2 film areas. Therefore major effort was given during the second year to the optimization of the rf sputtering process with studies of as-deposited film quality and ultimately cell fabrication and testing. During this year CdS was sputter-deposited for the first time. Completed cells were fabricated for the first time using rf sputtering for both the CdS and CdTe layers. LDPVD was used for the deposition of a $CdCl_2$ layer prior to the usual 400°C air anneal. For both laser-deposited cells and the rf sputtered cells, LOF SnO_2-coated soda-lime glass has

been used and our standard contact method has been a thin layer of copper followed by a gold cap.[3]

A considerable amount of materials characterization has been used to help optimize the deposition conditions. These include optical absorption, scanning electron microscopy with energy dispersive x-ray spectroscopy (SEM/EDS), x-ray diffraction, Raman scattering, photoluminescence (PL), electrial conductivity and Hall measurements. These efforts were supplemented by additional measurements performed at NREL (carrier lifetime, electron beam induced current) and at Colorado State U. (detailed solar cell loss analysis).

2.0 Advances in Film Deposition and Cell Fabrication Techniques

2.1 RF Sputtering

Cadmium telluride--RF sputtering of CdTe was begun in our laboratory near the end of the first year of contract work. During the second year we have achieved a first-order optimization of the deposition parameters relying primarily on results from SEM studies of as-deposited grain size and from photoluminescence (PL) measurements of the as-grown films. The deposition system was sketched in our first year annual report. The system is built around a two-inch planar magnetron rf sputter gun (AJA International) and employs turbo-molecular pumping. Typical growth conditions are: $P_{argon} \cong 5$ mT, argon flow = 10-15 sccm, rf power $\cong$ 100 Watts, $T_{substrate}$ = 375 °C. Sputtering was performed on-axis with a target-substrate distance of 7 cm. Growth rates were typically 3 Å/sec. Average grain size was ~0.25 μm for the as-grown films 1-1.5 μm thick. Characteristics of the CdTe films are further described in Section 4.2.

Cadmium sulfide--The growth of CdS films was begun in the summer of 1992. Again the growth conditions were optimized to first order with conditions similar to those for the sputter growth of CdTe films. However, we have found the growth rate to be somewhat slower for the same rf power--typically 1-2 Å/sec. A suitable growth temperature for CdS is about 250 °C and rf powers of ~200 W were typical. As expected for the lower growth temperature, the grain size was quite small (~0.1 μm or below). For both CdTe and CdS, films were grown on alkali-free glass (Corning 7059 or NEG 0A2) for most electrical and optical studies but also on SnO_2-coated soda-lime glass (mostly LOF 10 Ω/□, and some LOF 20 Ω/□). Raman, PL, SEM and other characterization results are given in Section 4.1.

Sputtered CdS/CdTe Solar Cells--Several solar cells were fabricated using rf sputtering for both CdS and CdTe layers. Because our system has only one sputter gun, CdS layers were first deposited on several LOF SnO_2-coated substrates, sputter targets were changed, and then CdTe layers were sputtered. Thus the CdS was exposed to air for some time between the CdS and CdTe depositions. No attempt was made to clean the CdS surface prior to the start of the CdTe deposition. The cells were completed by the deposition of a thin layer of $CdCl_2$ by means of LDPVD, annealed for 15 minutes at 400°C in air, and then contacted with a Cu/Au layer (30 Å/ 200 Å respectively). A 150 °C, 30 minute diffusion step completed the cell fabrication.

Details of cell measurements are provided in Section 3 below. One of these all-sputtered cells was tested by NREL and yielded an AM1.5 efficiency of 10.4% with good uniformity among the

~4 mm contacts across the ~7.5 cm x 7.5 cm film area. These cells had a relatively thick CdS layer (~0.7 μm thick) which was reflected in the spectral quantum efficiency measurements showing essentially no response below $\lambda = 520$ nm. (See Fig. 3-3 below.) To our knowledge, the only other recent work work using rf sputtering for CdS/CdTe cells was reported by Abou-Elfotouh, et al[4] who used sputtering only for the CdTe layer and produced a 6.7% cell.

Our results reported here appear to be the first in which both CdS and CdTe layers are sputtered and indicate considerable promise for the use of rf sputtering as a method for deposition of large area, thin-film CdTe-based photovoltaics.

2.2 Laser-Driven Physical Vapor Deposition

CdS and CdTe thin films--We have continued efforts to improve the materials quality of the individual films of CdS and CdTe grown by pulsed laser deposition. With the use of electrical measurements, PL, and SEM for materials characterization we have made slight adjustments in the film growth conditions. Thus we have increased the growth temperature from typically 280 °C to ~330°C and have used slightly higher laser power densities at the target surface. We have found that the first films grown from a freshly pressed target have moderate numbers of pinholes which appear to arise from "dust" ablated from the target. Although the size and density of pinholes are small enough and few enough (~30/mm^2 of diameter ≤ 20 μm) not to cause noticeable deterioration in the cell performance, we have found, nevertheless, that these pinholes can be almost entirely eliminated with a pulsed laser prescan of the target before the first film growth from a new target. We are presently beginning the use of sintered polycrystalline targets which are expected to remove such initializing problems.

We have attempted to introduce shallow dopants into CdTe during the laser deposition process; however, unlike for CdS, the doping efficiency appears to be low. Any changes in electrical conductivity are within experimental errors of being nonexistent. We have observed, with some types of dopants such as Cd_3Sb_2 added to the target before pressing, that there is some enhanced PL which may be evidence of some dopant activation. However, the effects are small.

CdS/CdTe Solar Cells--With the improved growth conditions, as determined from individual film properties, and from optimization of the two layer thicknesses, we have improved the cell efficiencies from 8.7% to 10.5% during the past year. Some of this improved performance arises from adjustments to the post-deposition treatments. We have continued to use LDPVD for deposition of a ~0.1 to 0.2 μm $CdCl_2$ layer without exposing the CdTe to air. We have found that a 15 minute anneal at 400°C in air is sufficient for optimizing the cell performance. In fact it appears that, for our optimized layer thicknesses of 0.1 μm CdS and 1.3 μm CdTe, a longer anneal leads to too much interdiffusion across the CdS/CdTe interface. The excessive interdiffusion is apparent in the PL spectra and also as a soft "turn-on" of photoresponse at wavelengths above 520 nm. (See data presented in Sections 3 and 4.)

Slight additional improvements were obtained by decreasing the thickness of the Cu layer in the evaporated Cu/Au contacts. We find that 30Å of Cu and ≥200Å of Au was optimum for our geometries and for the 1.3 μm CdTe layers. Diffusion/annealing steps (after metal deposition) of greater than 30 minutes at 150°C caused the cell performance to degrade.

These post-deposition treatments and contacting procedures were optimized for the LDPVD cells and we have used similar parameters for the fabrication of the sputter-deposited cells.

3.0 Cell Diagnostics and Performance

In this section we shall present the results of tests of cells fabricated during this contract year. Most of the results are from tests performed at NREL and emphasize results from the all-sputtered cells although some results are included from LDPVD cells.

3.1 Current-voltage characteristics

The I-V trace of a recently fabricated sputtered cell is shown in Fig. 3-1 and a similar trace from a recent LDPVD-grown cell is shown in Fig. 3-2. The sputtered cell has a CdTe thickness of 1.5 μm and a CdS thickness of 0.7 μm. The LDPVD cell has a CdTe thickness of 1.3 μm and a CdS thickness of 0.1 μm. This relatively thick CdS layer of the sputtered cell accounts for the low current of the sputtered cell. However, the voltage of the sputtered cell is quite good and the fill factor is good. Efforts are presently underway to optimize the CdS thickness and hopefully to improve the short-circuit current and thus the efficiency of the sputtered cell.

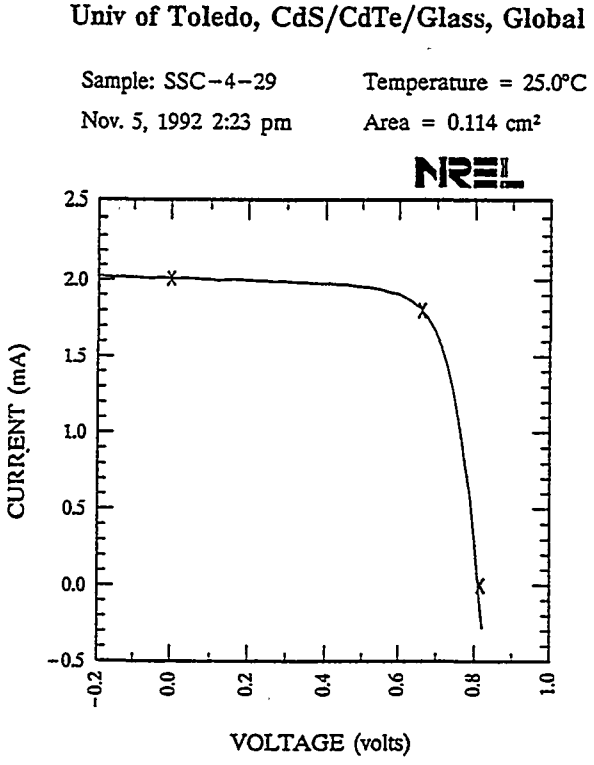

Fig. 3-1. I-V characteristic of all-sputtered cell SSC4-29. V_{oc}=0.8146 V, J_{sc}=17.61 mA/cm^2, FF=72.80%, eff=10.4%. (Data from K. Emery.)

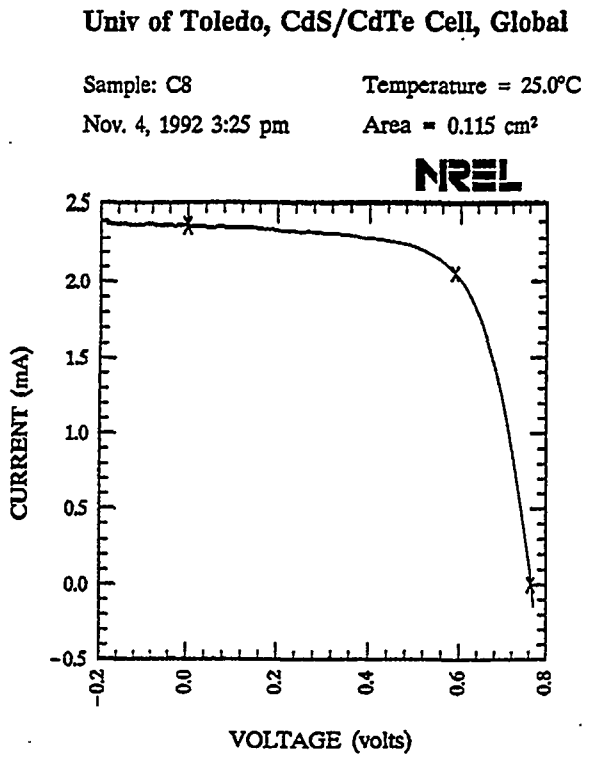

Fig. 3-2. I-V characteristic of all-LDPVD cell SC299-8. V_{oc}=0.7644 V, J_{sc}=20.69 mA/cm^2, FF=66.64%, eff=10.5%. (Data from K. Emery.)

3.2 Spectral quantum efficiency

The spectral quantum efficiency of a sputtered cell and an LDPVD cell are shown in Figures 3-3 and 3-4 respectively. Note that the two curves are normalized differently and have different wavelength scales. However, one may clearly notice the effect of the relatively thick CdS layer in the sputtered cell. In the region from 400 to 500 nm, the all-sputtered cell has almost no response due to absorption in the CdS region.

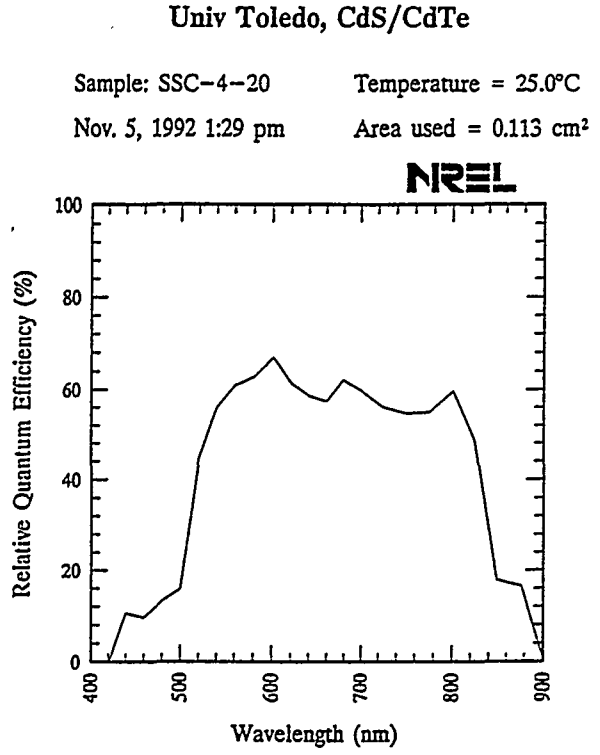

Fig. 3-3. Relative spectral quantum efficiency of cell SSC4-29. Light bias of 1.5 mA; no voltage bias. (From K. Emery.)

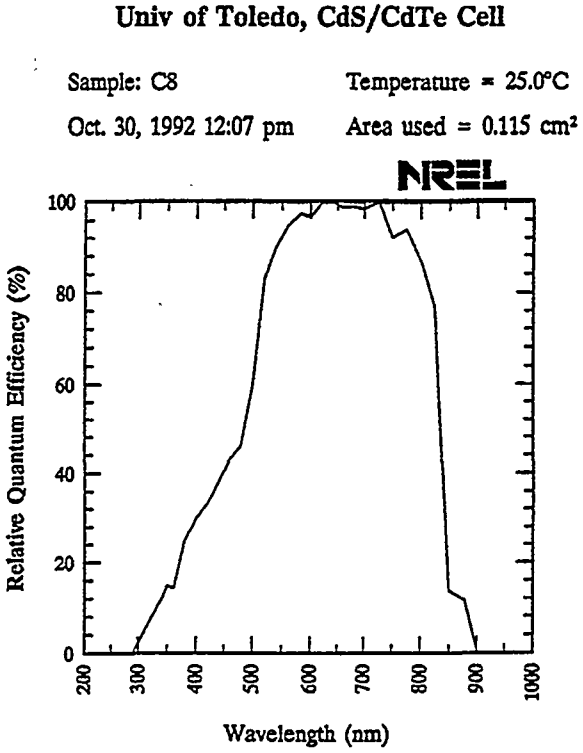

Fig. 3-4. Relative spectral quantum efficiency of cell SC299-8. Light bias of 0.5 mA; no voltage bias. (From K. Emery.)

3.3 Minority carrier lifetime

The photoluminescence decay lifetime at room temperature for the sputtered cell was measured in the laboratory of R.K. Ahrenkiel of NREL using excitation at 600 nm and detection at 820 nm. The initial fast exponential decay was measured from the CdTe at the CdS interface ("front surface") to be 0.5 nsec. The decay from the CdTe/air interface (back surface) adjacent to a contact was found to be 0.3 nsec. These lifetimes are noticeably shorter than best values reported for measurements on a 9% cell from Photon Energy[5] (with 6 μm thick CdTe) for which lifetimes of 5.67 ns and 2.0 ns were measured on the front and back interfaces respectively. (Grain sizes were typically 4 μm and 2 μm, respectively, at these surfaces.) Other measurements on cells from the U. of South Florida[6] (with CdTe thicknesses from 4-6 μm and grain size ~5 μm) have

given lifetimes ranging from 0.4 ns to 1.5 ns and no strong correlation with cell efficiencies which ranged from 10.5% to 13%. These data, therefore, indicate that there is room for improvement in the minority carrier lifetime of our rf sputtered CdTe but that the cell performance is probably not at this point limited by the carrier lifetime.

3.4 Electron beam induced currents

The electron beam induced current (EBIC) response has been measured at NREL by R. Matson for a region on the all-sputtered film near the ~4mm diameter contact which defines cell SSC4-29. In cross section from a fractured edge of the film, the current response reaches a maximum approximately 1/5 of the distance into the CdTe film from the CdS interface. (See Figure 3-5a.) Current collection extends almost completely to the back surface for this cell which had a CdTe thickness of ~1.0 μm. The EBIC response along the junction near the depth of maximum response in the CdTe is shown in Fig. 3-5b. There appears to be considerable variation in the current response, some of which may arise from the surface texture of the fractured edge but much of the variation presumably arises from variation in response from grain to grain.

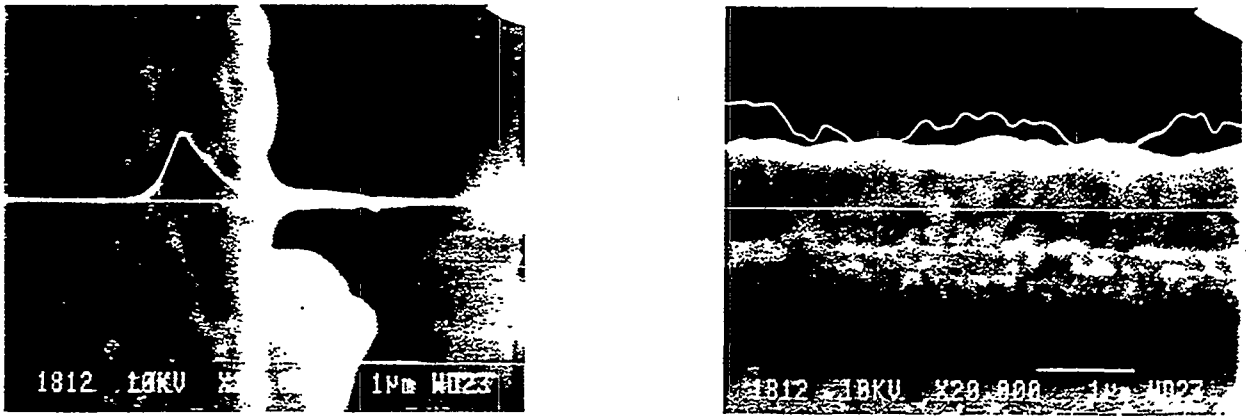

Fig. 3-5. a) EBIC response from an all-sputtered cell obtained from a fractured edge and scanned perpendicular to the junction. b) EBIC response from same cell scanned parallel to the junction near the depth of maximum current response.

3.5 Analysis of loss mechanisms

Prof. J.R. Sites has provided an analysis of loss mechanisms for an LDPVD cell (SC275-11) with slightly lower efficiency (10.2%) than discussed in Section 3.1 above. This laser-deposited cell tested at V_{oc} = 0.77 V, J_{sc} = 22 mA/cm^2, and fill factor of 0.60. This cell, deposited on 20 Ω/square LOF glass, showed a series resistance of 4 Ω at AM 1.5 and 8 Ω in the dark. Diode quality factors were 2.6 and 1.8, respectively in light and darkness. These numbers indicate that series resistance is the major loss mechanism[7] and that the large difference between forward and dark recombination suggests there is significant room for improvement in the junction quality.

4.0 Materials Quality

In this section we present the results of characterization measurements of the individual materials and interfaces particularly those which provide information on the relative quality (LDPVD vs sputtered) of the as-grown materials and the materials after post-deposition processing. The characterization techniques include: optical absorption, SEM, EDS, photoluminescence, Raman scattering, electrical resistivity, and Hall constant. Some data are also presented of measurements on samples from Solar Cells Inc (CdS and CdTe by vapor deposition) and from NREL (CdS by solution growth).

4.1 Cadmium sulfide

4.1.1 Photoluminescence

Photoluminescence (PL), especially low temperature PL, provides considerable information on the materials quality of CdS. The photoluminescence efficiency provides a qualitative measure of carrier lifetime and the location of particular emission bands and lines can help to identify impurities and defect states in the material. Raman scattering, when performed with laser photon energies above the band gap, may be considered as resonant photoluminescence and also can provide information on carrier lifetime. In addition, the width of the Raman lines is affected by grain size in the limit of very small sizes $\leq$ 100Å. We have studied CdS prepared by LDPVD, rf sputtering, vapor deposition, and solution growth, as well as bulk single crystals.

LDPVD film quality vs. target material--Figure 4-1 shows the PL spectra from three films grown by LDPVD with different targets. The targets were pressed pure CdS powder (Alpha Chemicals 5N), pressed In-doped CdS powder (Alpha 500 ppm CdS:In), and a single crystal high-purity CdS (Eagle Picher). Note that the film grown from single crystal CdS has much stronger band-edge luminescence and much weaker deep-level bands. The film grown from pressed powder shows dominating deep level emission bands in the range from 570 to 770 nm. These bands appear to be suppressed in the film grown from powder doped with 500 ppm In. For all of these ~1μm thick films the growth temperature was ~250 °C.

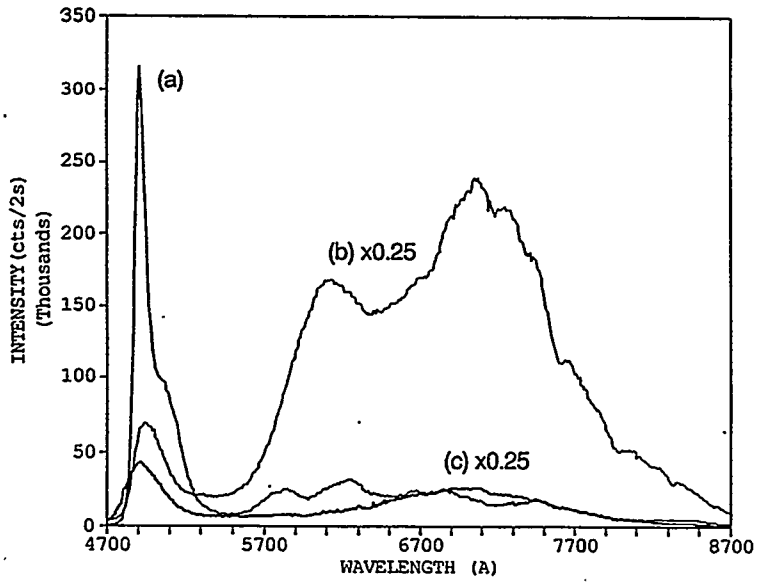

Fig. 4-1. 80 K photoluminescence from three CdS films grown by LDPVD at ~250 °C on Corning 7059 glass using different targets. a) single crystal CdS, b) pure CdS powder, and c) 500 ppm In-doped CdS powder. λ = 457.9 nm; in traces (b) and (c) scale is x0.25.

LDPVD films vs. growth temperature--The 80K PL spectra from LDPVD films grown from crystalline CdS targets (*cf.* Fig. 4-2) show the following general trends: Depositions onto room temperature substrates yield films with relatively weak PL. For depositions above room temperature, two prominent bands are seen--a near-band-edge peak at ~490 nm and a "deep level" band centered near 610 nm. Both bands increase in intensity with growth temperature to 320 °C but above 300 °C the deep level band grows more rapidly and the near-band-edge peak appears to broaden. Thus, temperatures near 250-270 °C appear to maximize the ratio of band-edge emission to deep-level emisssion. We speculate that above 270 °C there may be some movement away from stoichiometry leading to increased deep level centers responsible for the band at 610 nm.

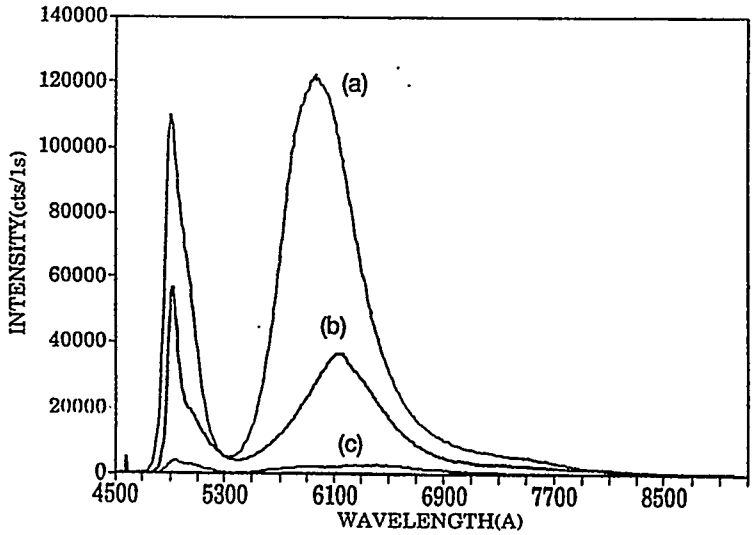

Fig. 4-2. 80K photoluminescence from several CdS films grown by LDPVD on NEG 0A-2 from a single crystal CdS target. Substrate temperatures: (a) 320 °C, (b) 270 °C, & (c) 30 °C. λ = 457.9 nm.

RF sputtered CdS--The growth temperature for rf sputtering of CdS was optimized to first order by tracking changes in the PL spectra. These changes are displayed in Fig. 4-3. Again the band-edge emission and the deep-level emission change dramatically as the growth temperature changes. For low temperature growth (e.g., room temperature) all PL is weak. As T_s rises, two broad deep level emission bands appear--one centered at 610 nm and the other near 710 nm. Both bands reach maximum intensity near 300 °C. The band edge emission (λ = 495 nm) optimizes in intensity at T_s = 350 °C, however, increasing the deposition temperature further to 420 °C appears to remove the band-edge emission in favor of a luminescent center at ~520 nm. These changes also appear to be correlated somewhat with increasing grain size and also indicate some decrease in density of deep-level recombination centers as the growth temperature increases from 250°C to 400°C. The maximum band-edge PL emission occurs near T_s = 350 °C which correlates well with the observations in LDPVD material. The principal difference with the sputtered films is the presence of a fairly strong red emission peaked at ~710 nm which extends into the near infrared. This broad band is very weak in the LDPVD material.

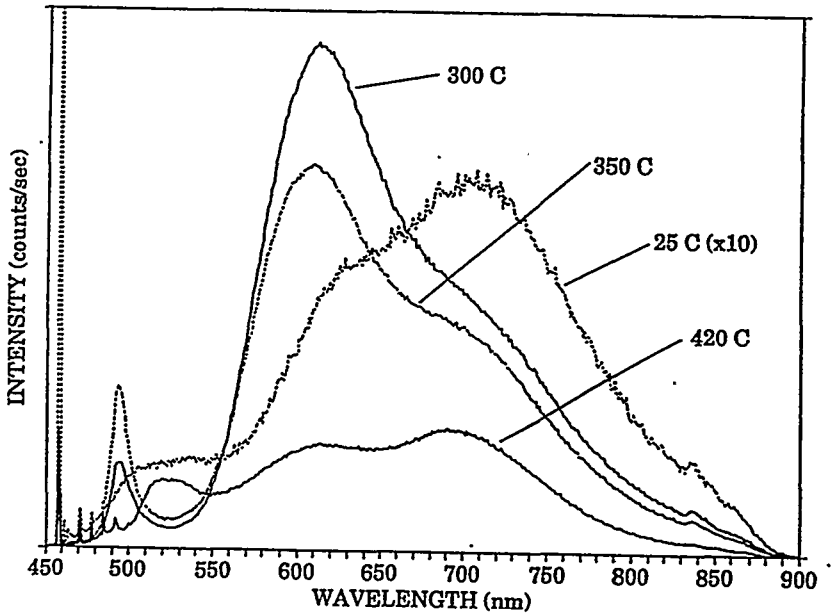

Fig. 4-3. PL spectra of sputtered CdS films grown on 10Ω LOF glass at a variety of substrate temperatures: 25 °C (data multiplied by 10), 300 °C, 350 °C, and 420 °C λ = 457.9 nm excitation.

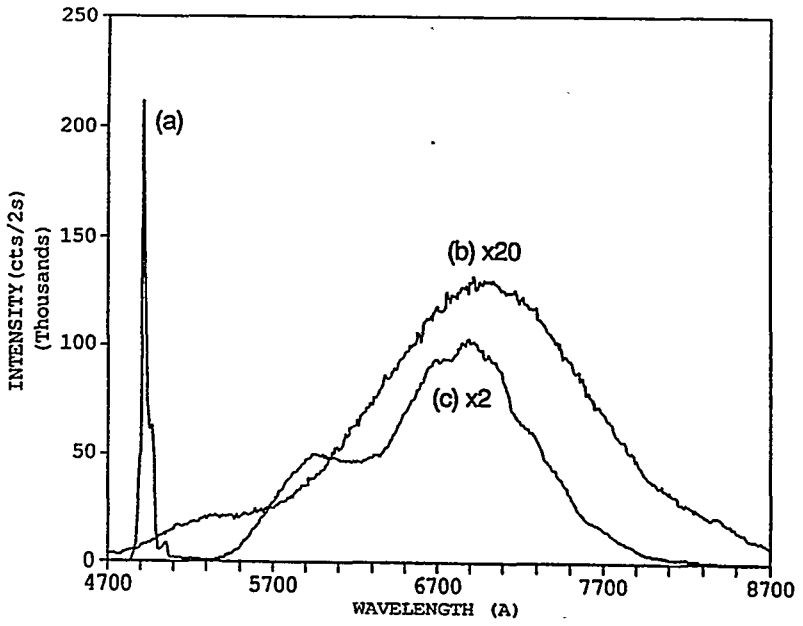

Fig. 4-4. 80K PL spectra of CdS prepared from a) bulk single crystal (Eagle-Picher), b) solution growth at 90 °C (NREL) [data multiplied by 20], and c) vapor deposition (Solar Cells Inc) [data multiplied by 2].

Films by other growth methods--Figure 4-4 shows for comparison the spectra from CdS prepared by three other growth methods. We show PL obtained from a film grown by vapor deposition with a substrate temperature of ~600 °C. Relatively little band-edge emission is seen but deep-level emission is very strong in two main bands at ~590 nm and ~690 nm. [Note that these bands are slightly blue-shifted from the two broad deep-level bands seen in the sputtered films.] The PL from a solution-grown film is extremely broad extending from the band edge into

the near infra-red (to the limits of the photomultiplier response). Finally, we show a comparison spectrum from the single crystal grown by vapor transport (which was the target for one of the films of Fig. 4-1 and the films of Fig. 4-2). Note the almost complete absence of deep-level emission in the region from 550 to 870 nm for the single crystal material.

Annealing of sputtered and LDPVD films--For both LDPVD and sputtered films the treatment with $CdCl_2$ and air annealing at 400°C changes the PL spectra considerably. (See Fig. 4-5.) The deep level band (centered near 700 nm) which was the strongest in the as-deposited films (sputtered and LDPVD grown from powder targets) is greatly reduced and a band near 590-610 nm is greatly enhanced in intensity (by x100 approximately). (Compare with Figs 4-1 and 4-3.) There appears to be little change in the near-band-edge emission following anneal. Note especially the large increase in deep-level emission for the films prepared from crystalline targets. These spectra indicate the presence of considerable densities of deep (~0.5 eV) radiative centers in the films treated similarly to those in the better solar cells.

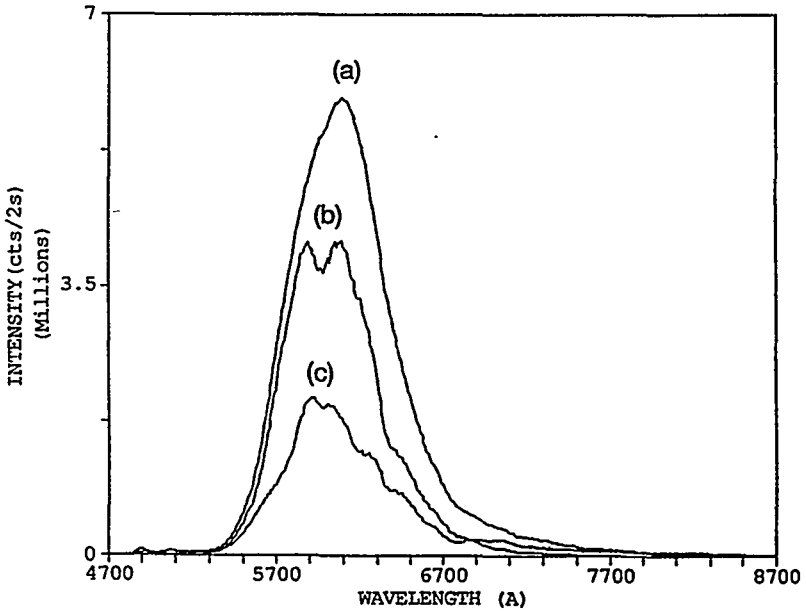

Fig. 4-5. 80K PL spectra of several LDPVD CdS films after $CdCl_2$ treatment and anneal in air at 400 °C for 40 minutes. Target material: a) single crystal, b) doped powder (500 ppm In), and c) pure (5N) powder; T_s = 250 °C; λ = 457.9 nm.

4.1.2 Raman measurements

In general for II-VI semiconductors, Raman scattering is very strong for photon energies slightly above the fundamental (direct) band gap. The Fröhlich-type electron-phonon interaction dominates the electron thermalization process and produces strong multiple-order "Raman" scattering which may also be considered as "hot" luminescence. In this sense the presence and strength of the multiple order phonon lines in the Raman spectrum gives a measure of the carrier lifetime. In addition, when the grain size is very small (~20 Å), significant broadening may be seen in the Raman lines. These effects have been studied extensively in III-V semiconductors.[8] Thus the Raman spectra tend to yield important information in the limit of small grain sizes and

in medium quality material for which the electron-phonon scattering time is comparable to the non-radiative decay lifetime due perhaps to deep impurity centers (radiative or nonradiative).

We have studied this behavior for several films of rf sputtered CdS and for a solution-grown film. Figure 4-6 shows spectra obtained for several CdS films sputtered at different substrate temperatures. Considerable broadening of the first order Raman line and even more broadening of the second order line occur at the lower growth temperatures. The solution-grown film has the broadest lines indicating the existence of a very small grain polycrystalline material or perhaps porous material. It should be recognized that random strain could also account for Raman line broadening but this does not seem plausible for these low temperature growths. A preliminary analysis of the broadening which includes the optic phonon dispersion near the Brillouin zone center indicates grain sizes as small as 35 Å for the solution grown film and 50 Å for the room temperature sputtered film. For growth temperatures above 200 °C, the Raman linewidths indicate grain sizes above 100 Å.

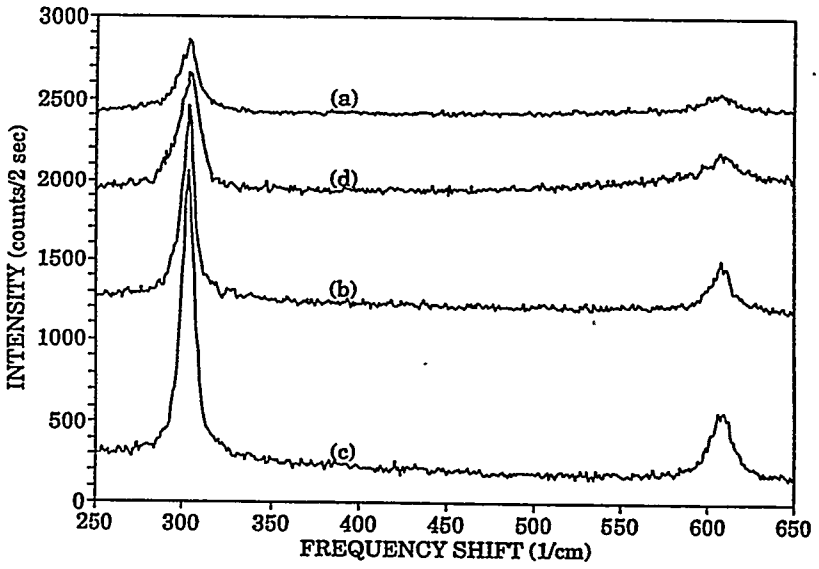

Fig. 4-6. Raman spectra of several as-grown films of CdS grown by rf sputtering on LOF (10Ω/□). Growth temperatures and [first-order Raman widths] are: a) T_s = 25 °C [10 cm^{-1}], b) T_s = 300 °C [8 cm^{-1}], c) T_s = 325 °C [8 cm^{-1}], and d) for a solution-grown film from NREL [13 cm^{-1}]. Instrumental resolution was 3 cm^{-1}.

4.1.3 SEM studies of grain size (CdS and CdTe)

Scanning electron microscopy studies of grain size in CdS for the higher temperature growths indicate that the grains are larger for the sputtered films than for the LPDVD films grown at the same temperature.[9] The data are shown in Fig. 4-7. Grain size is a strong function of temperature, but assuming good substrate temperature calibration in the different growth chambers, the sputter growth appears to facilitate larger grains. We speculate that this may arise from the impact of energetic neutral and ionized species from the plasma on the growing film surface.

The data of Fig. 4-7 on CdTe grain size D vs growth temperature may be interpreted in terms of an enthalpy of activation ΔH_g (during growth) using the relationship[10]

$$D \sim R^{-\beta} \exp(\Delta S/k) \exp(-\Delta H_g/kT)$$

where D is the maximum grain size, R is the growth rate, β is a constant, ΔS is the entropy of activation. The data yield

$$\Delta H_g = 0.13 \pm 0.03 \text{ eV} \quad \text{(CdTe growth)}.$$

In addition, we have studied the effect of post-deposition anneals on the CdS grain size. These results are shown in Fig. 4-8. The data on average grain size D have been fit with the function[11]

$$D^2 = 4\alpha\gamma t[((f\lambda\nu V_a)/kT) \exp(\Delta S/k) \exp(-\Delta H_a/kT)$$

where α is a constant, γ is the interfacial energy per unit area, f is the accommodation probability, λ is the boundary thickness, ν is the vibrational frequency, and V_a is the atomic volume. The enthalpy of grain boundary movement from Fig. 4-8 is found to be

$$\Delta H_a = 0.94 \pm 0.10 \text{ eV} \quad \text{for CdS annealing, and}$$

$$\Delta H_a = 0.53 \pm 0.07 \text{ eV} \quad \text{for CdTe annealing.}$$

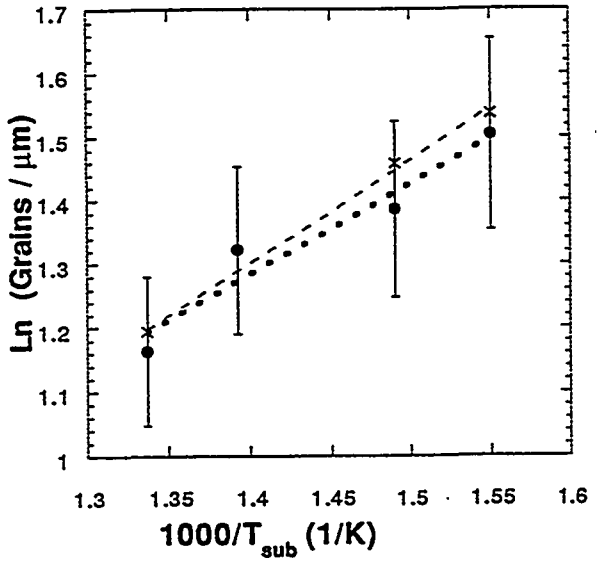

Fig. 4-7. Average grain sizes as inferred from plan view micrographs of rf sputtered CdTe films (as-grown), for two different thicknesses: • = 0.67 μm, and x = 0.33 μm.

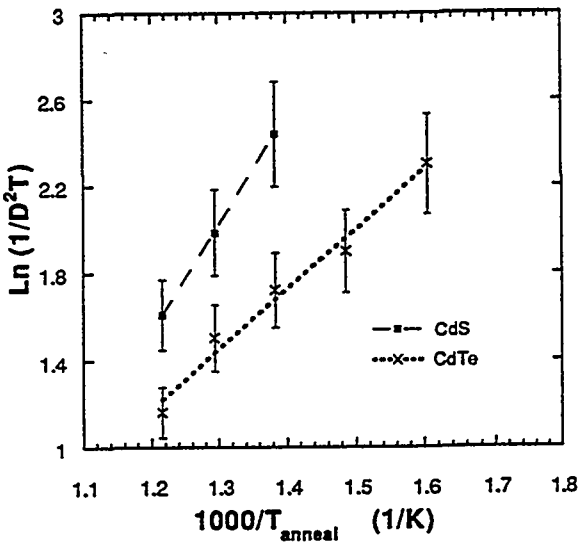

Fig. 4-8. Average grain size as a function of anneal temperature for LDPVD CdS and CdTe films. 30 minute anneals in air without $CdCl_2$ treatment.

Comparison of the data of Figure 4-7 with those of Fig. 4-8 clearly show the much lower activation enthalpy during growth compared with post-growth anneal. The data of Fig. 4-8 show the significantly lower enthalpy of grain boundary movement for CdTe compared with CdS during post-growth anneal. This follows the known bond strengths of these semiconductors.

4.1.4 Electrical conductivity of LDPVD CdS (before and after anneal)

The electrical conductivity of three types of CdS films were studied in detail. The films were grown by LDPVD from targets of 1) single crystal CdS, 2) pressed pure CdS powder, and 3) pressed In-doped CdS powder (500 ppm In). Electrically the films from pure CdS targets appear very similar and the target composition and structure seem to make little difference. Room temperature resistivities for the as-grown films are around 1000 Ω-cm. Doping with In reduces the resistivity, which quickly saturates near 0.05 Ω-cm, with the most rapid change occurring between 0 and 0.1% In. (See Fig. 4-10.) The light sensitivity also decreases rapidly with the addition of In and Fig. 4-11 indicates that the carrier concentration increases by about three orders of magnitude as the In concentration increases and seems to saturate at about $10^{19}/cm^3$ above 0.2% In. It would appear that undoped or lightly doped films (≤0.1%) would result in CdS films of higher resistivity and higher light sensitivity which should be more suitable for photovoltaic applications. It should be noted however, that these results are for as-grown films (by LDPVD) and measurements on $CdCl_2$-treated films indicate increased resistivity and light-to-dark ratio after treatment and 400 °C anneal in air. Our Hall measurements show that the resistivity increase after anneal is primarily due to a reduction in carrier concentration.[12]

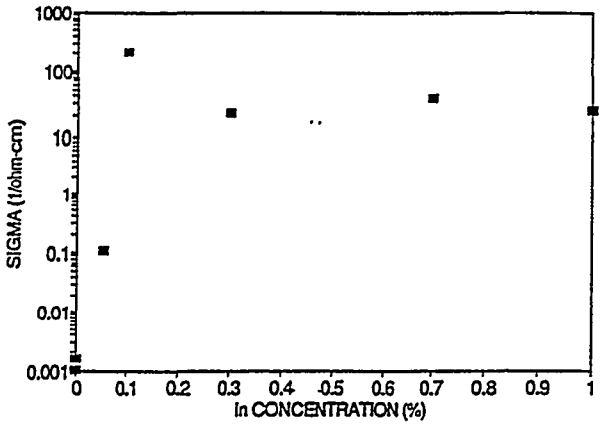

Fig. 4-9. Room temperature dark conductivity of CdS films grown by LDPVD at 250 °C from targets with various atomic % In concentrations mixed with CdS powder before pressing.

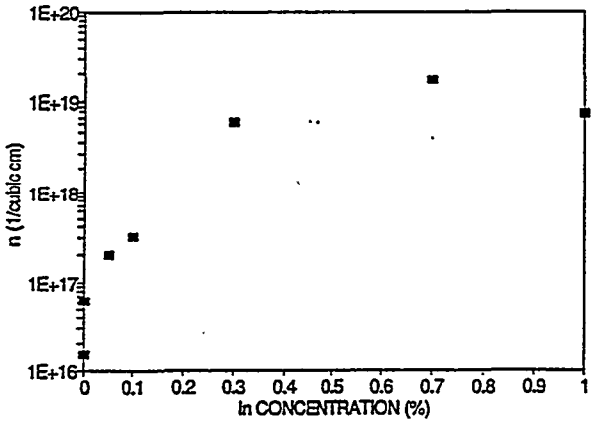

Fig. 4-10. Room temperature carrier density of same CdS films as for Fig. 4-9.

4.2 Cadmium telluride

4.2.1 Photoluminescence and Raman

As is the case for CdS, photoluminescence of CdTe provides much information on the film quality. However, because the band gap is quite near the long wavelength end of the photocathode response of our GaAs(Cs) photomultiplier (λ_{max} = 900 nm), we are unable to obtain as much information on the deep level radiative centers in CdTe as we can on CdS. Nevertheless, the PL shows excellent sensitivity to adjustment of various growth parameters such as deposition temperature, grain size, and deposition method. PL behavior as a function of several of these parameters is discussed below.

Dependence on T_s for LDPVD films (pure CdTe)--With the use of the Kr laser line at 752.5 nm, which lies only about 40 meV above the band edge of CdTe at 80 K, it is possible to observe both resonant Raman scattering and near-band-edge photoluminescence from CdTe films. Figure 4-11 displays these spectra for four films deposited by LDPVD from pressed powder targets on alkali-free glass substrates at temperatures ranging from 245 °C to 320 °C. We have found that photoluminescence out to 890 nm is very weak for films grown from pure CdTe targets by LDPVD. (Sputtered pure CdTe shows stronger PL as seen in Fig. 4-14 below; and LDPVD films with dopants may exhibit much stronger PL as seen in Fig. 4-12,13 below.) However, the Raman scattering (first order peak and three overtones) clearly shows increasing intensity, particularly for the overtones, as the deposition temperature increases. This is a consequence of increasing carrier lifetime at the higher deposition temperatures. (It is difficult to increase still further the deposition temperature since the growth rate decreases rapidly above 320 °C.)

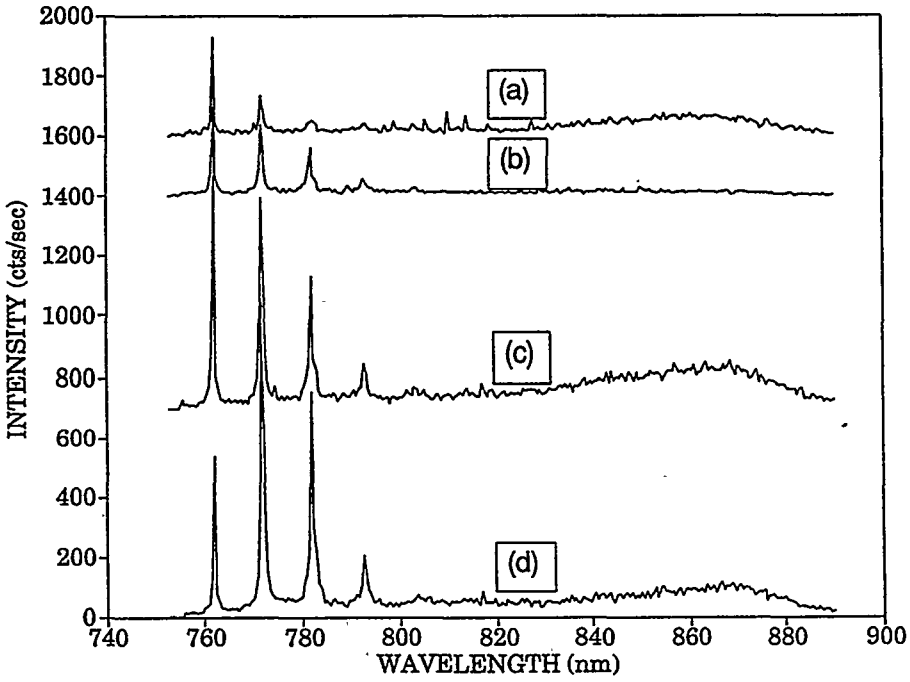

Fig. 4-11. 80 K PL from LDPVD CdTe films on Corning 7059 glass for substrate temperatures of a) 245 °C, b) 280 °C, c) 300 °C, and d) 320 °C. λ = 752 nm.

Dependence on target composition--Similarly, the PL is sensitive to changes in the composition of the target used for the LDPVD growth. We prepared a variety of pressed powder targets with excess Cd and with a variety of dopants (As, P, and Sb). The most successful of the dopants was Sb; however, for this dopants we used the compound Cd_3Sb_2 and it is quite possible that the additional Cd is important in enhancing the PL. Fig. 4-13 shows the results for films grown from Cd_3Sb_2-doped CdTe targets for a series of substrate temperatures. Two distinct PL bands are seen--a band-edge emission at about 780 nm (which lies under the Raman lines) and a band at 850 nm which is ~130 meV into the band gap. Both of the features appear to optimize for T_s near 400 °C. In Fig. 4-14 we show the PL from films grown from targets prepared with excess Cd. It appears the the PL can be enhanced with excess Cd almost as well as with the Cd_3Sb_2 dopant.

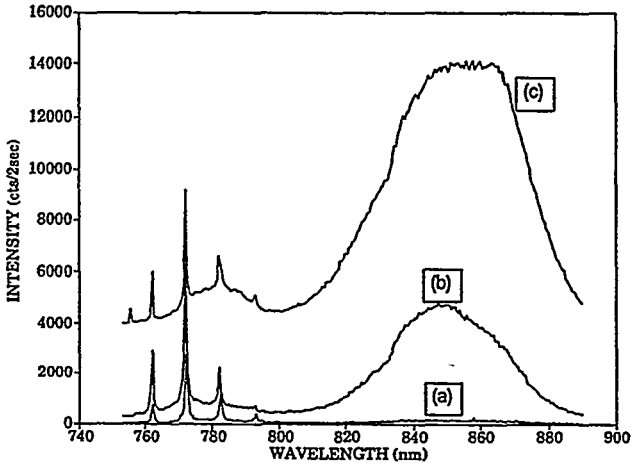

Fig. 4-12. 80 K PL from LDPVD CdTe films on Corning 7059 glass deposited from targets mixed with Cd_3Sb_2 powder. λ = 457.9 nm; trace a) T_s = 250 °C, b) 300 °C, and c) 400 °C.

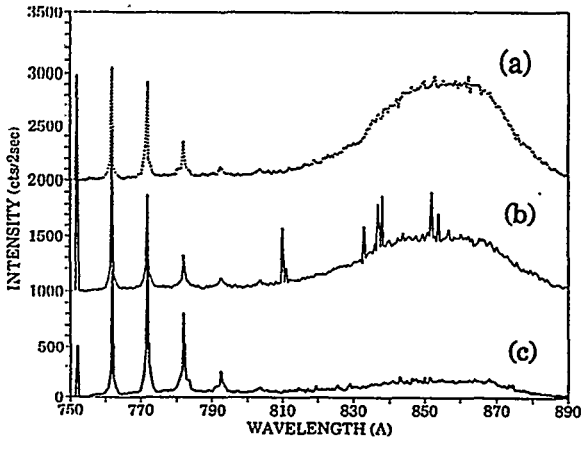

Fig. 4-13. 80 K PL from LDPVD CdTe films on Corning 7059 glass deposited from 0.1% Cd-doped CdTe targets for substrate temperatures of a) 370 b) 385 and c) 400 °C. The narrow peaks for λ>810 nm are laser plasma emission lines.

Dependence on T_s for sputtered films (pure CdTe)--The rf sputtered films tend to show stronger PL than the LDPVD films grown from pure CdTe powder. PL spectra from as-deposited sputtered films are shown in Fig. 4-14. Again strong Raman scattering can be seen superimposed on band-edge emission and deep-level bands which are somewhat broader than for the LDPVD-grown material doped with either excess Cd or Cd_3Sb_2. The film grown at 400 °C shows the strongest band-edge emission as well as the strongest deep-level band.

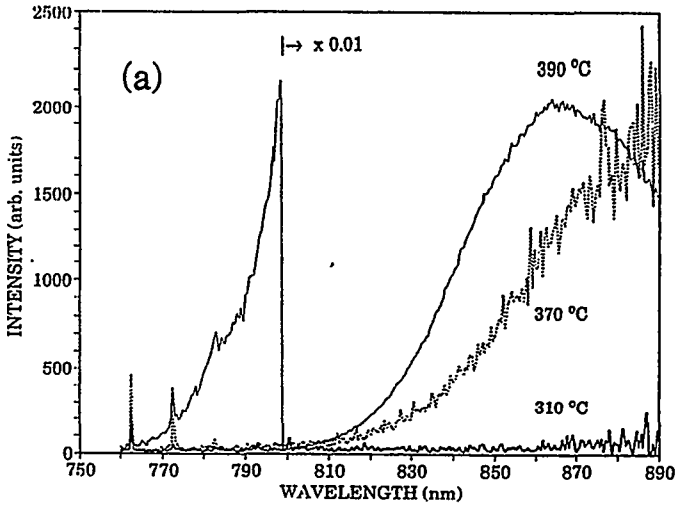

Fig. 4-14 80K PL from rf sputtered CdTe films on 7059 Corning glass for several deposition temperatures. Panel a) films grown at 11 cm target-substrate separation; panel b) films grown at 7 cm. Data taken with λ = 752 nm. Note: in this figure data have been corrected for diminishing photomultiplier response at long wavelengths.

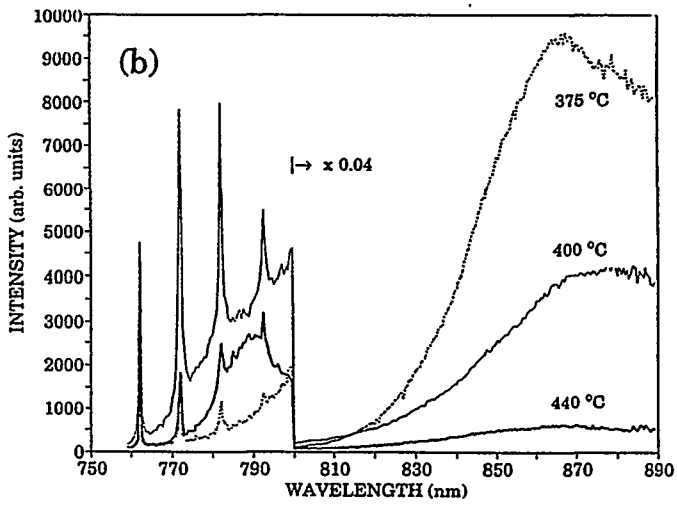

PL changes in LDPVD and sputtered CdTe films after $CdCl_2$ treatment--After the laser deposition of a thin $CdCl_2$ layer and heat treatment at 400 °C for 15 minutes, there is a strong increase in the deep level PL signal (>x100 increase) and little change in the band-edge intensity. The data are shown in Fig. 4-15.

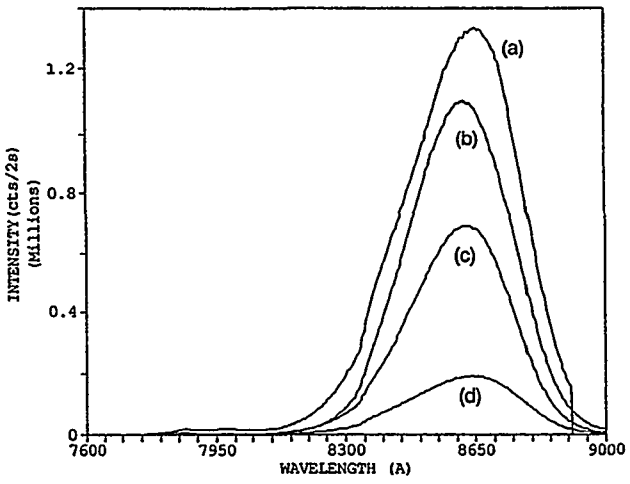

Fig. 4-15. 80K PL spectra from $CdCl_2$-treated and 400 °C annealed CdTe films. λ = 752 nm. Trace a) sputtered, b) LDPVD from crystal CdTe, c)LDPVD from pure powder, and d) LDPVD from 0.3% CdSb-doped CdTe powder.

4.2.2 SEM studies of grain size for as-grown, sputtered films

The average grain size for rf sputtered films of CdTe was measured from SEM micrographs for a range of films grown at different substrate temperatures. The data were shown in Fig. 4-7. The grain size appears to saturate at about 0.25 μm for these films which were approximately 1.3 μm thick.

4.2.3 Electrical conductivity (before and after annealing)(LDPVD and sputtered)

All of the CdTe samples were of high resistivity (~10^8 Ω-cm) with grain sizes typically 0.1 μm for the LDPVD films and up to 0.25 μm for the sputtered films. The $CdCl_2$-treatment increased the grain size and reduced the resistivity. The most dramatic change is seen in the light sensitivity, where an order-of-magnitude increase is seen in the light-to-dark ratio after annealing.[11]

4.3 CdS/CdTe interfaces

Photoluminescence from the interface--One of the most powerful aspects of Raman scattering and photoluminescence is the capability of probing buried interfaces. The most important region for the performance of the CdTe solar cell is the CdS/CdTe interface, which is at or near the active n/p junction. Other studies of optical properties[13] and PL[14] of the interface region have been reported. We have extended this work by using several different excitation wavelengths. Thus, with excitation at 457.9 nm and 80K sample temperature the laser excites the CdS to a depth of about 100Å and generates strong CdS band-edge and deep-level emission as seen in Fig. 4-17a.

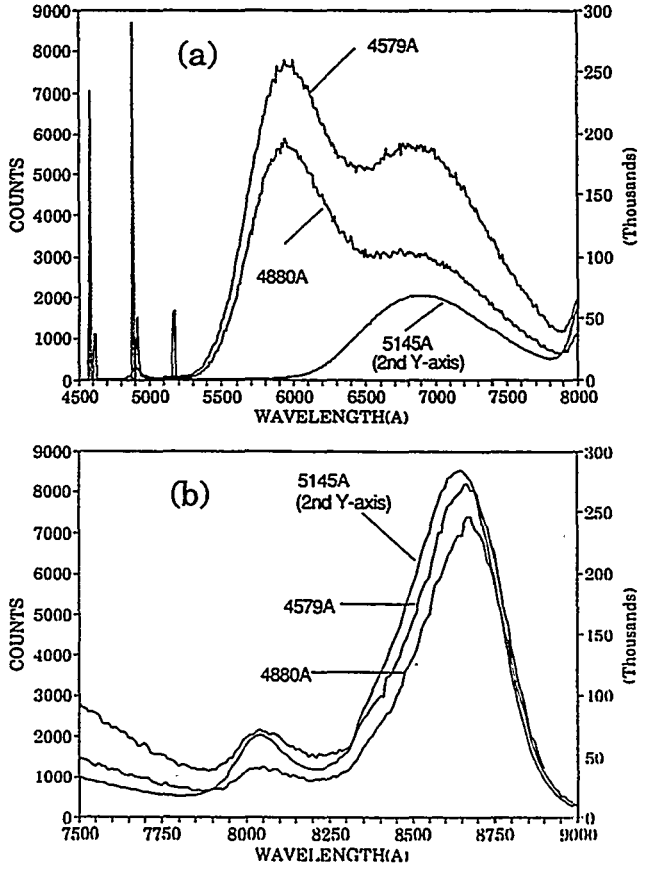

Fig. 4-17. Panel (a) shows the predominantly CdS-like PL and panel (b) shows the predominantly CdTe-like PL obtained with the laser entering through the glass/SnO_2 layers. The strong wavelength-dependent effects result from differing absorption in the CdS layer. Data taken at 80 K; films grown by LDPVD, treated with $CdCl_2$, and annealed at 400 °C.

However, with excitation at 514 nm the CdS is almost transparent to the laser which is strongly absorbed in the CdTe at the interface (~100 Å deep). The 514 nm spectrum in Fig. 4-17a, shows some weak deep level emission from CdS (or CdSTe alloy) and the long wavelength part of the spectrum (Fig. 4-17b) shows very strong near-band-edge and deep level emission fromthe CdTe at the interface. The 488 nm spectrum shows intermediate behavior. This is illustrated in panels (a) and (b) of Fig. 4-17 divided according to that part of the spectra showing mainly CdS PL and that showing mainly CdTe PL.

During annealing at 400 °C (following $CdCl_2$ treatment) there is significant interdiffusion across the original CdS/CdTe interface. The effects of interdiffusion are shown dramatically in Fig. 4-18 which shows the effects of $CdCl_2$ treatment and anneal on four different pieces of a single LDPVD solar cell structure. The pieces had differing CdS layer thicknesses (0.05, 0.1, and 0.15 μm) and were annealed in air for either 15 minutes or 40 minutes. For the longer anneal time the ~600 nm CdS band decreases while the ~700 nm band undergoes a relative increase. This is probably a result of the in-diffusion of Te from the CdTe side of the interface. The strongest CdTe PL relative to the CdS PL is obtained from the sample with the 0.05 μm thick CdS (measured for the as-deposited film).

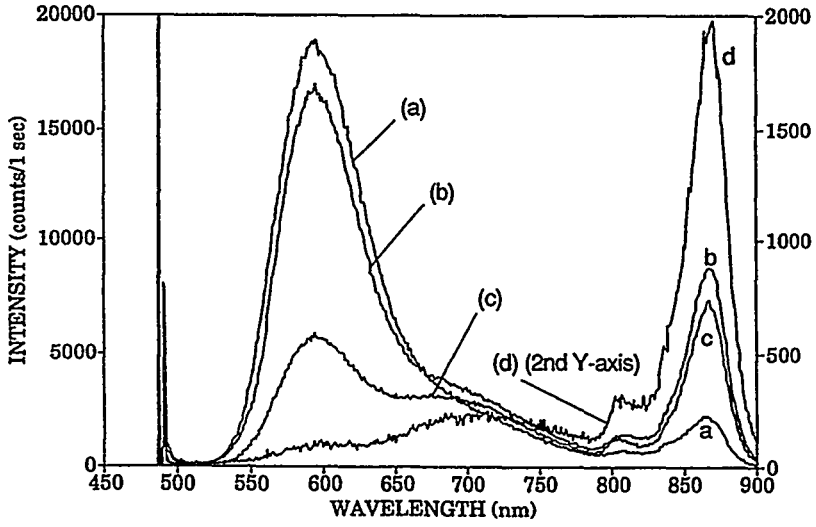

Fig. 4-18. 80K PL spectra obtained with λ = 488 nm and laser excitation through the glass/SnO_2/CdS layers. CdS thicknesses of a) 0.15 μm, b) 0.1 μm, c) 0.1 μm, and d) 0.05 μm. Anneal times of 15 minutes for a), b), and d); 40 minutes for c).

Finally, the interdiffusion at the CdS/CdTe interface also influences the PL from the CdTe. To study these effects without possible deep-level PL from the CdS we used the Kr laser line at 752 nm. Fig. 4-19 compares the spectrum obtained from the interface (laser incident through the glass/SnO_2) with that obtained from the CdTe/air interface. This was taken after the normal solar cell processing. (The CdTe/air interface was probed adjacent to the Cu/Au contact spot.

Changes in SQE due to interdiffusion--The interdiffusion across the original CdS/CdTe interface, which is displayed in the PL spectra of Figs. 4-17, 4-18, and 4-19, also affects the spectral response of the solar cell. Fig. 4-20 displays the spectral quantum efficiency (SQE) of two cells which received the 400 °C heat treatments for 15 minutes and for 40 minutes. The more extensive diffusion which occurs after the 40 minute anneal shows up as a slow "turn-on"

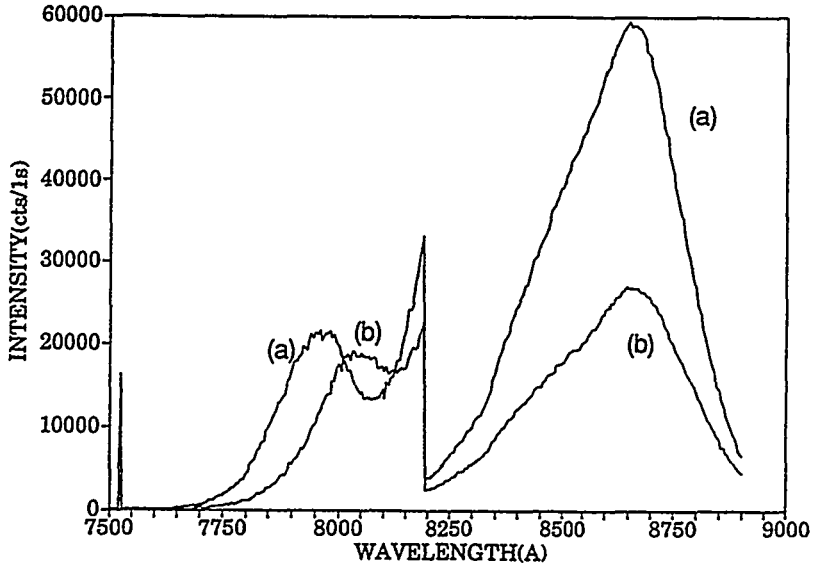

Fig. 4-19. 80 K PL spectra from a solar cell structure obtained from a) CdS/CdTe interface and from b) CdTe-/air interface. Laser excitation at 752 nm. Data multiplied by x 10 below 8200 Å.

of the cell response as the wavelength increases beyond 500 nm and a slightly extended red response. There appears to be some trade-off in red response for blue response. Unfortunately, the CdS and CdTe layer thicknesses of the two cells were slightly different so that comparisons of V_{oc} and overall efficiency are difficult. Further work is planned to study these effects. This is probably due to the interdiffusion and formation of CdS_xTe_{1-x} alloys of varying composition.[13,14] Presumably the minority carrier collection is poor in the alloy region although the absorption is significant due to the lowering of the band gap as a consequence of alloying. This reduction of band gap is enhanced by the large "band bending" which occurs in this alloy.[15]

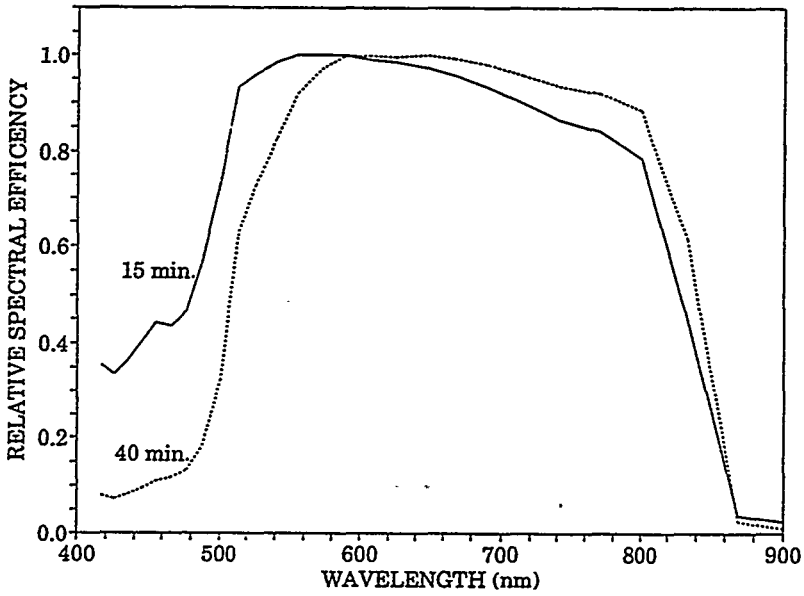

Fig. 4-20. SQE responses of two similarly prepared LDPVD CdS/CdTe solar cells but with anneal times of a) 15 minutes and b) 40 minutes. Curves are independently normalized at the point of maximum response.

4.4 ZnTe by rf sputtering and Cu doping effects

In collaboration with Solar Cells Inc, we have made a series of rf magnetron sputter depositions of ZnTe films. These films have been grown at a variety of substrate temperatures and with Cu doping by adding pieces of metallic copper foil on the target surface. Incorporation of Cu in the films is clearly indicated by SEM/EDS measurements although the concentration has not been quantified. Hall measurements on these films clearly indicate electrical activity of the Cu. Carrier concentrations range from $5 \times 10^{17}/cm^3$ for nominally undoped films to $2 \times 10^{21}/cm^3$ for the heaviest doping. Efforts are still underway to optimize the deposition parameters for producing films suitable for PV applications as a top contacting material to CdTe.

5.0 Substrate temperature measurements (LOF and Corning 7059)

5.1 Measurements of IR absorption and reflectivity

Over the past year we have used principally two types of substrates--alkali-free glass 1mm thick (Corning 7059 and NEG 0A2) and SnO_2-coated soda-lime glass (principally 10 Ω/square "low-E" glass from LOF). In both the sputter and LDPVD deposition chambers the substrate is heated radiatively from above while the film is deposited on the lower side. In this configuration, we have found that the heating characteristics of these two types of substrates are significantly different. Since the lower side of the substrates radiates essentially to the room-temperature chamber walls, the equilibrium temperature depends strongly on the emissivity of the lower surface. The SnO_2-coated glass has a much lower emissivity in the infrared. We measured the optical properties of both glass in response to a ~500 °C heater. The net power absorbed is not greatly different (70% for Corning 7059 and 86% for 10 Ω/□ LOF glass) but the net emissivity (1-reflectivity) to this radiation is very much different (93% for Corning 7059 and 30% for 10Ω/□ LOF glass). As a result, the LOF glass radiates less effectively and therefore reaches a higher equilibrium temperature for the same heater power. Table 5.1 exhibits the results of our measurements on the two types of glass.

Table 5.1 I.R. reflection, transmission and absorption of typical substrates.

Substrate	Radiation Incident	Refl.	Trans.	Abs.
LOF 10Ω/□	on SnO_2	0.70±0.07	0.03±0.01	0.27±0.06
	on glass	0.11±0.01	0.03±0.01	0.86±0.02
Corning 7059		0.07±0.01	0.23±0.05	0.70±0.05

5.2 Ruby fluorescence measurements of substrate temperature

In order to measure the glass temperature with a non-contact probe (and thereby avoid problems of heat flow through the probe) we utilized small chips of ruby crystal bonded to the substrate at different positions. The ruby R-line fluorescence, excited with a weak argon laser beam at 514.5 nm, yielded a convenient record of the substrate temperature.[16] Two typical fluorescence spectra are shown in Fig. 5-1. Ruby fluorescence is a standard pressure calibration technique and it also has been calibrated for temperature shift.[16] The results of the ruby fluorescence measurements are displayed in Fig. 5-2 which shows the substrate temperature as a function of heater power for substrates in the sputter chamber. The solid curve through the points is the theoretical equilibrium substrate temperature, fit with one arbitrary constant, assuming radiative cooling from the lower surface only. Note that the SnO_2-coated glass reaches a significantly higher equilibrium temperature. The equation for the glass temperature is

$$T_s = \text{const}\,[T_R^4 + (P/\varepsilon\sigma A)]^{1/4},$$

where T_R is the temperature of the chamber walls, P is the heater power, ε is the emissivity of the bottom surface of the substrate, and σ is Stefan's constant.

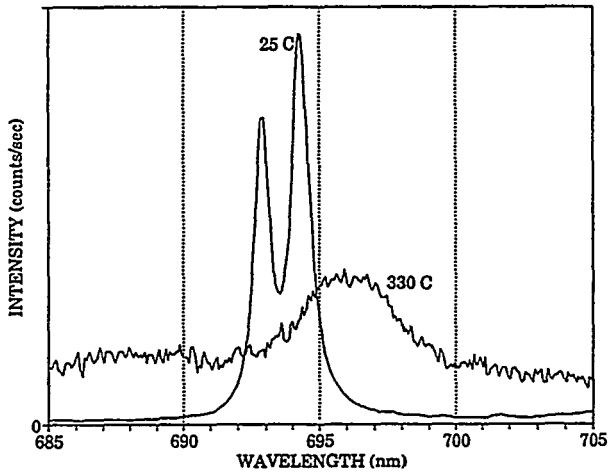

Fig. 5-1. Fluorescence spectra from a ruby chip mounted on a glass substrate in the rf sputter chamber for two substrate temperatures.

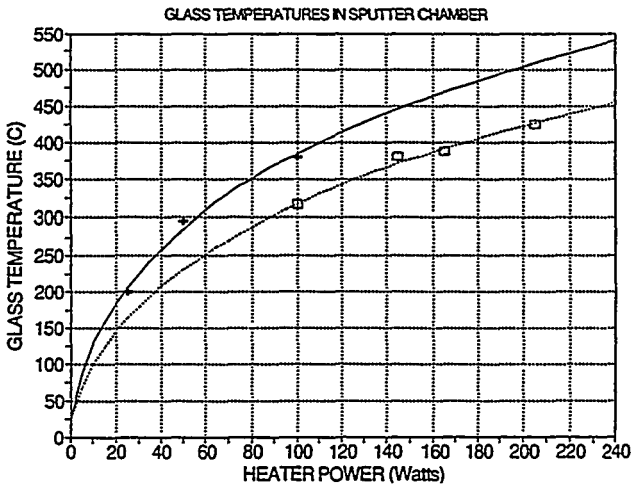

Fig. 5-2. Substrate temperature as inferred from ruby fluorescence as a function of heater power for LOF 10Ω/□ (solid curve) & 7059 glass (dotted curve).

6.0 Summer NSF student projects

During the summer of 1992, the University of Toledo Department of Physics and Astronomy hosted 12 undergraduate students participating in research projects as part of the NSF-sponsored Research Experiences for Undergraduates (REU) program.[17] Three of these students participated in projects which benefitted this NREL-sponsored work. We were very pleased with all three of these students and their 10 week research collaborations were of considerable benefit to our work. We also feel that their participation in photovoltaic research as undergraduates has stimulated their continuing interest in PV research and development. The three students are

Kristina McNett from Ohio University in Athens, OH; Brett Miller from Miami Univ. in Ohio, and Jay Whitacre from Oberlin College in Oberlin, OH. A brief summary is provided below of highlights of their activities.

6.1 Optical beam induced current scanning (Jay Whitacre)

Jay Whitacre completed the instrumentation of this system, begun by a UT undergraduate student, Ann Wagonner, last year. The system scans a solar cell under a focussed HeNe, Argon, or GaAs laser beam with a resolution of ~15 μm while monitoring the cell current. Examples of his work are shown in Figures 6-1 and 6-2. In Fig. 6-1 is presented an optical micrograph of a ~3mm diameter cell which has three sizeable "dead" areas. The topographical map clearly correlates with the dark areas from the optical image. In Fig. 6-2 are shown two other cells with a comparison between the I-V curves of the cells and a three dimensional image of the OBIC current response. Note that the cell with the very poor I-V curve actually has some regions which have very good current response. We anticipate scaling up this system in the near future to accommodate larger PV submodules.

Fig. 6-1. Optical micrograph of a solar cell with visible defects (pinholes, scratches).

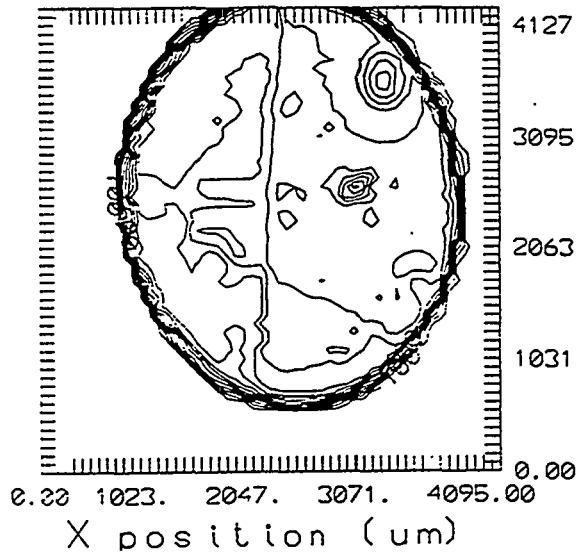

Fig. 6-2. OBIC topograph of same cell as for Fig. 6-1 showing spatially resolved current response.

6.2 Calibration of PL spectrometer and SQE measurements (Tina McNett)

A major thrust of the work of Tina McNett was to carry out efficiency calibrations of the triple spectrometer used for Raman and photoluminescence and also to calibrate the spectral quantum efficiency system. She used a tungsten-halogen lamp with intensity calibration traceable to NIST standards. We currently use her results to correct PL data to remove the spectrometer and detector sensitivity variations with wavelength.

6.3 Electrical measurements (Brett Miller)

Brett worked closely with Prof. Bohn making electrical conductivity measurements of CdS and CdTe films using both a strip line geometry and the vander Pauw geometry. He also performed some temperature-dependent Hall measurements. Many of these results have been described earlier in this report.

7.0 Conclusions

During the past year considerable progress has been made in improving the performance of CdS/CdTe solar cells based on both LDPVD and rf sputtering. In the case of rf sputtering, we have been able to achieve rapid progress partly by relying on process parameters optimized for the LDPVD process. The first rf magnetron sputtered films were grown in our laboratory in Oct 1991 and the first sputtered CdS films in August 1992. By the end of October 1992 we have reached cell performance which indicates considerable promise for the sputtering method. High open-circuit voltage (0.814 V) and good fill factor (72.8%) were achieved. The short circuit current was relatively low (17.61 mA/cm^2) but appears to be due to the thick CdS layer which has not been optimized. At this point it is quite clear that, in comparison with rf sputtering, the laser driven deposition process is not well suited for the large area depositions needed for thin-film photovoltaics. However, the flexibility inherent in the LDPVD process and the similarity to rf sputtering continue to make LDPVD highly useful for testing new target materials and for preliminary optimization of deposition parameters.

Considerable effort has been placed on photoluminescence, Raman, SEM, and Hall characterization of the individual films. These characterization tools have provided important guideposts for optimizing the individual film quality. In addition, the PL and Raman are being use quite successfully to examine the properties of the CdS/CdTe interface and to track the extent of interdiffusion during the post-deposition heat treatments.

The use of LDPVD for applying the $CdCl_2$ without liquid solvents prior to the annealing treatment has proved very reliable and yields very reproducible results.

Fluorescence from ruby chips mounted on the glass substrates has given a good calibration of the substrate temperature without requiring contacting probes.

Finally, preliminary studies have been done on rf sputtering of Cu-doped ZnTe in collaboration with Solar Cells Inc which indicate considerable promise for this technique.

8.0 Future Directions

During the next year our efforts will be directed largely toward optimization of the parameters for rf magnetron sputtering of CdS and CdTe with the goal of further improvements in cell performance. Thorough studies will be conducted of the dependence of CdTe and CdS film properties and growth rates on gas pressure and flow rate during sputtering. The LDPVD process will be used in support of the sputtering effort. As film quality improves, greater effort will be

placed on improved electrical contact performance as well as the replacement of gold as a contacting material.

9.0 Acknowledgments

We indebted to K. Emery for the device measurements, R. Matson for EBIC measurements, R.K. Ahrenkiel for photoluminescence decay measurements, and to J.R. Sites for analysis of loss mechanisms. In addition, we are especially grateful to Bolko von Roedern and also to Harin Ullal for many helpful discussions and encouragement.

10.0 References

1. A. D. Compaan, R.G. Bohn, A.Aydinli, A. Bhat, C. M. Tabory, L-H. Tsien, S. Liu, M. Shao, M. Savage, and Y. Li, "Thin Film Cadmium Telluride Photovoltaic Cells," Annual Report, Photovoltaic Program, FY 1991. (March 1992). NREL/TP-410-4724. 306pp. Available NTIS: Order NO. DE 92001248.

2. A. Compaan and A. Bhat, "Laser-Driven Physical Vapor Deposition for Thin-Film CdTe Solar Cells," Int'l J. Solar Energy, 20, no 1-4 (1992).

3. B.N. Baron, R.W. Birkmire, J.E. Phillips, W.N. Shafarman, S.S. Hegedus, and B.E. McCandless, "Fundamentals of Polycrystalline Thin Film Materials and Devices" Final Report to SERI July 1990 (Institute of Energy Conversion, Univ. of Delaware, Newark, Delaware, 19716)

4. F. Abou El-Fotouh, M. Soliman, A.E. Riad, M. Al-Jassim, and T. Coutts, "Preparation and Characterization of Polycrystalline rf Sputtered CdTe Thin Films for PV Application," 22nd IEEE Photovoltaic Specialists Conference-1991, (Las Vegas, Oct 7-11, 1991) p. 1109.

5. R. K. Ahrenkiel, B. M. Keyes, L. Wang, and S. P. Albright, "Minority-Carrier Lifetime of Polycrystalline CdTe in CdS/CdTe Solar Cells," 22nd IEEE Photovoltaic Specialists Conference-1991, (Las Vegas, Oct 7-11, 1991) 941 (1992).

6. B. M. Keyes, K. A. Emery, and R. K. Ahrenkiel, "Minority-Carrier Lifetime of Compound Semiconductors: Polycrystalline CdTe," Photovoltiac Advanced Research and Development Project [AIP Conference Proceedings 268], (Denver, May 1992) p. 149 (1992).

7. J. R. Sites, private communication

8. P. Parayanthal and F. H. Pollak, "Raman Scattering in Alloy Semiconductors: "Spatial Correlation" Model," Phys. Rev. Letters, 52, 1822 (1984); K. K. Tiong, P. M. Amirtharaj, F. H. Pollak, and D. E. Aspnes, Appl. Phys. Lett. 44, 122 (1984); H. Richter, Z. P. Wang, and L. Ley, Sol. State Commun. 39, 625 (1981).

9. M. Shao, R. G. Bohn, Y. Li, C. Tabory, Bull. Am. Phys. Soc, 37, 557 (1992).

10. J. Lopez-Otero. J. Cryst. Growth, 42, 157 (1977).

11. M. Shao, M.S. Thesis, The Univ. of Toledo (1992) (unpublished).

12. B. Miller and R. G. Bohn, Electrical Transport Properties of CdS and CdTe Thin Films, NSF-REU Grant PHY-9200403 report (1992) (unpublished).

13. I. Clemminck, M. Burgelman, M Casteleyn, J. De Poorter and A. Vervaet, "Interdiffusion of CdS and CdTe in Screenprinted and Sintered CdS-CdTe Solar Cells," 22nd IEEE Photovoltaic Specialists Conference-1991 (Las Vegas, Oct 7-11, 1991) p. 1114.

14. C.W. Tang, et al, J. Appl. Phys. 55, 3886 (1984); T.L. Chu, "Thin Film Cadmium Telluride, Zinc Telluride, and Mercury Zinc Telluride Solar Cells," final technical report to NREL for the period 7/1/88--12/31/91. p.38.

15. K. Ohata, J. Saraie, and T. Tanake, Jpn. J. Appl. Phys. 12, 1642 (1973).

16. R. A. Forman, G. J. Piermarini, J. D. Barnett, and S. Block, Science 176, 284 (1972); D. D. Ragan, R. Gustavsen, and D. Schifferl, J. Appl. Phys, 72, 5539 (1992); J. Yen and M. Nicol, J. Appl. Phys. 72, 5535 (1992).

17. Summer research work of Kristina McNett, Brett Miller, and Jay Whitacre supported in part by NSF-REU Grant No. PHY-9200403.

11.0 Publications

Refereed papers published:

1. A. Compaan, A. Bhat, C. Tabory, S. Liu, M. Nguyen, A. Aydinli, L-H. Tsien, and R. G. Bohn, "Fabrication of CdTe Solar Cells by Laser-Driven Physical Vapor Deposition," Solar Cells, 30, 79, 1991.

2. A. Aydinli, G. Contreras Puente, A. Bhat, and A. Compaan, "$ZnSe_xTe_{1-x}$ Films Grown by Pulsed Laser Deposition," J. Vac. Sci. & Technol. a 9, 3031 (1991).

3. A. Aydinli, A. Compaan, G. Contreras-Puente and Alice Mason, "Polycrystalline $Cd_{1-x}Zn_xTe$ Thin Films on Glass by Pulsed Laser Deposition," Sol. St. Commun. 80, 465 (1991).

4. A. Compaan, A. Bhat, C. Tabory, S. Liu, Y. Li, M.E. Savage, M. Shao, L. Tsien, and R.G. Bohn, "Polycrystalline CdTe Solar Cells by Pulsed Laser Deposition," Proc. 22nd IEEE Photovoltaic Specialists Conference-1991, 957 (1991) [Las Vegas, NE, Oct. 1991].

5. A. Compaan and A. Bhat, "Laser-Driven Physical Vapor Deposition for Thin-Film CdTe Solar Cells," Int. J. Solar Energy, 12, (1992).

6. A. Compaan, R.G. Bohn, A. Bhat, C. Tabory, M. Shao, Y. Li, M.E. Savage, and L. Tsien, "Thin-Film CdTe Photovoltaic Cells by Laser Deposition and RF Sputtering," PV AR&D Project AIP Conference Proceedings #268 (ed. by R. Noufi) p. 255. [NREL Photovoltaics Advanced Research and Development 11th Review Meeting, Denver, May 13-15, 1992].

Annual Reports published in SERI/NREL Annual Report, Photovoltaic Subcontract Program:

1. A. Compaan, R.G. Bohn, A.Aydinli, A. Bhat, L. Tsien, S. Liu, Z. Chen, and C. Tabory, "Thin Film Cadmium Telluride Photovoltaic Cells and Submodules Fabrication," Annual Report, Photovoltaic Program, FY 1990. (March 1991). SERI/TP-211-3643. Available NTIS: Order NO. DE 90000318.

2. A. D. Compaan, R.G. Bohn, A. Aydinli, A. Bhat, C. M. Tabory, L-H. Tsien, S. Liu, M. Shao, M. Savage, and Y. Li, "Thin Film Cadmium Telluride Photovoltaic Cells," Annual Report, Photovoltaic Program, FY 1991. (March 1992). NREL/TP-410-4724. 306pp. Available NTIS: Order NO. DE 92001248.

3. A. D. Compaan, R.G. Bohn, C.N. Tabory, M. Shao, Y. Li, Z. Feng, A. Fischer, and L-H. Tsien, "Thin Film Cadmium Telluride Photovoltaic Cells," Annual Report, Photovoltaic Program, FY 1992. (to be published)

Papers and Talks presented:

L. Tsien, R. G. Bohn and A. D. Compaan, Bull. Am. Phys. 36, 556 (1992), "Transport Properties of CdS Films Grown by Pulsed Laser Deposition."

A. Aydinli, Y. Rajakarunanayake, Y. Luo and A. Compaan, Bull. Am. Phys. Soc. 36, 559 (1992), "ZnSe and ZnTe Epitaxial Layers Grown by Laser-Driven Physical Vapor Deposition."

Y. Luo, Y. Rajakarunanayake, and A. Compaan, Bull. Am. Phys. Soc. 36, 559 (1992), "Time Resolved Light Emission and Ion Current Measurements from Pulsed Laser Generated II-VI Semiconductor Plumes."

A. Bhat, C. Tabory, S. Liu, Y. Li, M. E. Savage and A. Compaan, Bull. Am. Phys. Soc. 36, 559 (1992), "Pulsed Laser Deposition for CdTe Solar Cells."

Y. Li, C. Tabory, M. Shao, N. Lavalle and A. Compaan, Bull. Am. Phys. Soc. 36, 559 (1992), "Copper Doping of ZnTe Thin-Films Grown by Pulsed Laser Deposition."

C. Tabory, N. Lavalle, Y. Li, M. Savage, M. Shao, R. G. Bohn and A. Compaan, Bull. Am. Phys. Soc. 36, 559 (1992), "Optical And Electrical Properties of CdTe Thin Films Grown by Pulsed Laser Deposition and rf Sputtering."

M. E. Savage, U. Jayamaha, A. Aydinli, D. Shen and A. Compaan, Bull. Am. Phys. 36, 711 (1992), "Raman Studies of B-, P-, and C-Alloyed Excimer-Laser-Annealed a-Si."

12.0 Students and Visitors Participating in the Project

Students:

Ajit Bhat
Ph.D. March 1992 — "Thin Film Preparation Using Pulsed Laser Deposition"

Marc Savage
M. S. Dec 1992 — "Raman Studies of Heavily Doped Polycrystalline Si Films Prepared by Excimer-Laser Annealing of Doped a-Si:H"

Yuxin Li
M.S./Ph.D. in progress

Li-Hua Tsien
Ph.D. September 1992 — "Electrical Transport Properties of Polycrystalline CdS Films Produced by Laser-Driven Physical Vapor Deposition for CdS/CdTe Solar Cells"

Meilun Shao
M.S. August 1992 — "SEM and EDS Studies of CdTe and CdS Films Grown by LDPVD and RF Sputtering"

Zhirong Feng
M.S./Ph.D. in progress

Andreas Fischer
M.S./Ph.D. in progress

Technical Assistants:

Charles N. Tabory

Nicolas Lavalle (part-time)

Document Control Page	1. NREL Report No. NREL/TP-451-5813	2. NTIS Accession No. DE94000201	3. Recipient's Accession No.

4. Title and Subtitle

Thin Film Cadmium Telluride Photovoltaic Cells

5. Publication Date

October 1993

6.

7. Author(s)

A.D. Compaan, R.G. Bohn

8. Performing Organization Rept. No.

9. Performing Organization Name and Address

University of Toledo
Department of Physics
Toledo, Ohio 43606

10. Project/Task/Work Unit No.

PV331101

11. Contract (C) or Grant (G) No.

(C) ZN-1-19019-3

(G)

12. Sponsoring Organization Name and Address

National Renewable Energy Laboratory
1617 Cole Blvd.
Golden, CO 80401-3393

13. Type of Report & Period Covered

Technical Report
1 November 1991 - 31 October 1992

14.

15. Supplementary Notes

NREL technical monitor: B. von Roedern

16. Abstract (Limit: 200 words)

This report describes work to develop and optimize radio-frequency (RF) sputtering and laser-driven physical vapor deposition (LDPVD) for CdTe-based thin-film solar cells. Both of these techniques are vacuum-based and share several other common physical principles. However, they differ somewhat in the typical kinetic energies of Cd, Te, and S that impact on the growth surface. The values of several processing parameters—optimized with the LDPVD technique—were taken as starting values for the RF sputtering method. We completed an initial optimization of the sputtering parameters for the CdTe growth and also successfully sputtered CdS for the first time. In addition, we successfully fabricated what we believe are the first CdS/CdTe cells in which RF sputtering was used for both CdS and CdTe layers. We achieved an all-LDPVD cell with an air mass (AM) 1.5 efficiency of 10.5% and an all-RF-sputtered cell with AM 1.5 efficiency of 10.4%, as tested by NREL.

17. Document Analysis

a. Descriptors

thin film ; cadmium telluride ; photovoltaics ; solar cells

b. Identifiers/Open-Ended Terms

c. UC Categories

273

18. Availability Statement

National Technical Information Service
U.S. Department of Commerce
5285 Port Royal Road
Springfield, VA 22161

19. No. of Pages

32

20. Price

A03